J Chem Crystallogr (2012) 42:639–644
DOI 10.1007/s10870-012-0275-z

COMMUNICATION

Crystal Structures of (3*R*,3a*R*,4*S*,7*R*,7a*S*)-3-(Allyloxy)hexahydro-4,7-epoxyisobenzofuran-1(3*H*)-one and (3*S*,3a*R*,4*S*,7*R*,7a*S*)-3-((*E*)-But-2-en-1-yloxy)hexahydro-4,7-epoxyisobenzofuran-1(3*H*)-one: Confirmation of NMR Predicted Stereocentre Geometry

Mark Tarleton · Paul V. Bernhardt · Adam McCluskey

Received: 1 August 2011 / Accepted: 17 January 2012 / Published online: 8 February 2012

Abstract Crystal structures of two isomeric norcantharidin derivatives (3R,3aR,4S,7R,7aS)-3-(allyloxy)hexahydro-4,7-epoxyisobenzofuran-1(3*H*)-one (**7b**), and (3S,3aR,4S,7R,7aS)-3-((*E*)-but-2-en-1-yloxy)hexahydro-4,7-epoxyisobenzofuran-1(3*H*)-one (**8a**) have been determined. In both instances the equivalent enantiomer was also obtained. The crystal structures of these compounds clarify the stereochemistry inferred only by NMR analysis before.

Keywords Norcantharidin · Conformation · Crystal structure · Stereocentre

Introduction

Cantharidin (**1**) (Fig. 1) is a naturally occurring toxin found in over 1,000 species of blister beetles. Used by the Chinese as a natural remedy for the past 2,000 years, cantharidin has a long history as a therapeutic agent [1, 2]. The anti-cancer potential of cantharidin (**1**), was first recorded in 1,264 [1, 3]. Structurally simple, cantharidin (**1**) displays a number of features amenable to lead development including exhibiting no myelosuppresion and not being a substrate for the P-glycoprotein efflux pump. Despite this, the dose limiting nephrotoxicity has prevented cantharidin's entry into Western medicine [1, 2, 4]. Notwithstanding this, norcantharidin (**2**) (Fig. 1), the demethylated analogue, displays the favourable anti-cancer properties of cantharidin but displays little to no nephrotoxicity [1, 5]. In addition to the anti-cancer properties, both cantharidin and norcantharidin are potent inhibitors of the serine/threonine protein phosphatases PP1 and PP2A. Cantharidin is a 1.78 and 0.26 μM potent PP1 and PP2A inhibitor, respectively, while norcantharidin returns IC_{50} values of 1.98 and 0.37 μM for PP1 and PP2A, respectively [6].

Over the past decade we and others have expended considerable effort in the development of a better understanding of the key structural features that are required for both protein phosphatase inhibition and the anti-cancer effects of these analogues [6–22]. In the course of one such study we re-discovered, Novo-6 (**3**) (Fig. 1), a product that arose form the hydrogenation of 5,6-dehydronorcantharidin first reported by Eggelte [23]. Novo-6 (**3**) is phosphatase inactive, but does display remarkable anti-cancer selectivity with preferential cell death of colon cancer derived cell lines [6]. Excited by this observation, we have been keen to develop these analogues further, but our rational drug design approaches have been significantly hampered by the unknown stereochemistry at the C3-OH. The synthetic chemistry utilised in the preparation of Novo-6 suggests that there are two possible diastereomers, **3a** and **3b** (Scheme 1, enantiomers shown in boxed section).

Our initial efforts revealed only one diastereomer by TLC whereas those of Eggelte et al. showed the presence of two diastereomers by TLC [23]. This suggested that we could separate **3a** (anti) from **3b** (syn) by flash chromatography. We also note that our and Eggelte's efforts also suggest the presence of a major and minor product [23]. This is in keeping with the expected approach of the anhydride C=O to the surface of the Pd–C catalyst where the 7-O bridgehead would prefer to be distal with respect to the catalyst surface allowing a closer approach of the

M. Tarleton · A. McCluskey (✉)
Chemistry, School of Environmental and Life Sciences, University of Newcastle, Callaghan, NSW 2308, Australia
e-mail: Adam.McCluskey@newcastle.edu.au

P. V. Bernhardt
School of Chemistry and Molecular Biosciences, University of Queensland, Brisbane, QLD 4072, Australia

anhydride C=O to the surface. This occurs with the 7-O up (Fig. 2). Approach with the 7-O down places the anhydride C=O more distant to the surface thus disfavouring hydrogenation (Fig. 2). Our analysis suggests a 6:1 ratio of major:minor isomers (the actual ratios vary depending on the nature of the ether substituent). The positive identity of the major and minor diastereomers has been accomplished by derivatisation as an ether and crystallisation.

Experimental

Materials

All starting materials were purchased from Aldrich Chemical Co. and Lancaster Synthesis. Solvents were bulk, and distilled from glass prior to use, with the exception of THF which was freshly distilled from sodium-benzophenone. Reaction progress was monitored by TLC, on aluminium plates coated with silica gel with fluorescent indicator (Merck 60 F_{254}) and flash chromatography was conducted on Merck silica gel 60 (230–400 mesh). ^{1}H and ^{13}C spectra were recorded on a Bruker Avance AMX 300 MHz spectrometer at 300.13 and 75.48 MHz, respectively. Spectra were recorded using deuterated chloroform ($CDCl_3$) and chemical shifts are relative to TMS as internal standard. Melting points were recorded using a Büchi melting point M-565 apparatus and are uncorrected.

Synthesis

Compounds **7a** and **7b** (Scheme 2) were prepared by adding allyl alcohol (0.06 g, 1.07 mmol) to a magnetically stirred solution of Novo-6 (**3**, 0.20 g, 1.18 mmol) and catalytic *p*-TsOH (0.01 g) in anhydrous THF. The resulting solution was treated under microwave radiation for 1 h at 80 °C and 150 W. The reaction was then concentrated in vacuo and the residue was purified by flash chromatography (2:8 EtOAc:Hexanes) to yield an unseparated mixture of the diastereomers **7a** and **7b**. Slow evaporation of the eluate led to preferential crystallisation of **7b**. Analogue **7a** was obtained by concentration of the mother liquor.

7a: yield 59 mg, 26%, mp 36–38 °C, ^{1}H NMR ($CDCl_3$): δ 5.89 (m, 1H), 5.30 (d, $J = 1.7$ Hz, 1H), 5.28 (m, 2H), 4.83 (d, $J = 4.6$ Hz, 1H), 4.69 (d, $J = 4.6$ Hz, 1H), 4.30 (m, 1H), 4.07 (m, 1H), 2.92 (d, $J = 8.0$ Hz, 1H), 2.53 (dd, $J = 1.6$, 8.0 Hz, 1H), 1.85–1.46 (m, 4H) ppm; ^{13}C NMR ($CDCl_3$): δ 175.5, 132.3, 118.0, 105.8, 79.6, 79.0, 69.7, 50.3, 49.7, 28.0, 27.3 ppm.

7b: yield 18 mg, 8%, mp 100 °C, ^{1}H NMR ($CDCl_3$): δ 5.87–5.60 (m, 1H), 5.56 (d, $J = 6.8$ Hz, 1H), 5.37–5.23 (m, 2H), 5.13 (d, $J = 4.8$ Hz, 1H), 4.92 (d, $J = 4.8$ Hz, 1H), 4.46–4.40 (m, 1H), 4.17–4.10 (m, 1H), 2.89 (d, $J = 8.4$ Hz, 1H), 2.72–2.68 (m, 1H), 1.86–1.71 (m, 2H), 1.57–1.43 (m, 2H) ppm; ^{13}C NMR ($CDCl_3$): δ 174.8, 132.5, 117.7, 102.4, 78.7, 76.0, 70.8, 51.1, 46.6, 27.6, 27.5 ppm.

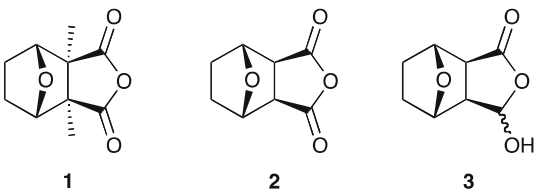

Fig. 1 Chemical structures of cantharidin (**1**), norcantharidin (**2**), and Novo-6 (**3**)

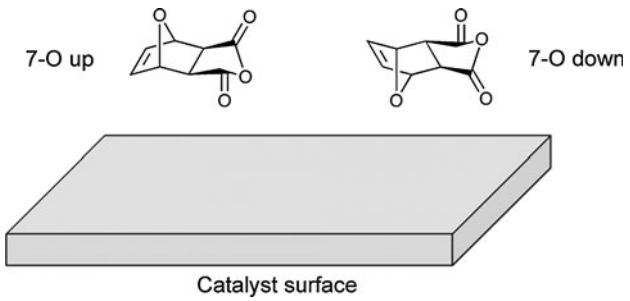

Fig. 2 Schematic representation of the approach of the two most likely approach configurations of **6** to the catalyst surface

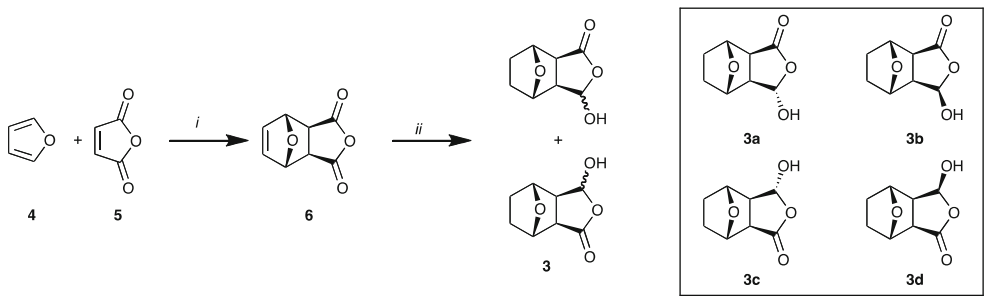

Scheme 1 Reagents and Conditions: *i* Et_2O, rt, 48 h; *ii* Pd–C, H_2 (4 atm), wet EtOH

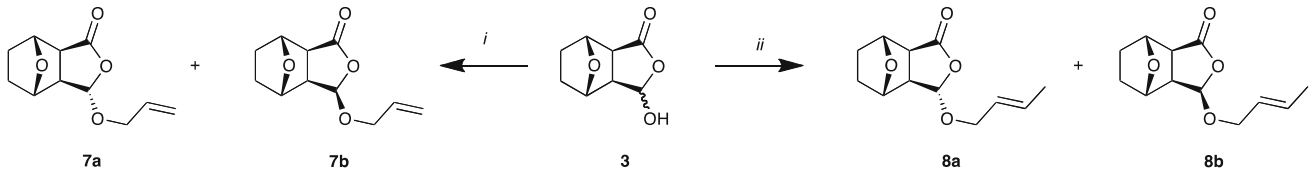

Scheme 2 Reagents and conditions *i* THF, pTsOH, allyl alcohol, MW 80 °C, 180 W, 1 h; *ii* THF, pTsOH, crotyl alcohol, MW 80 °C, 180 W, 1 h

Compounds **8a** and **8b** were prepared by adding crotyl alcohol (0.08 g, 1.07 mmol) to a magnetically stirred solution of Novo-6 (0.20 g, 1.18 mmol) and catalytic p-TsOH (0.01 g) in anhydrous THF. The resulting solution was treated under microwave radiation for 1 h at 80 °C and 150 W. The reaction was then concentrated in vacuo and the residue was purified by flash chromatography (1:9 EtOAc:Hexanes) to yield the corresponding isomers. Slow evaporation of the eluting solvents achieved preferential crystallisation of **8a** in this case. Isomer **8b** was obtained by concentration of the mother liquor.

8a: yield 100 mg, 42%, mp 78 °C, ^{1}H NMR ($CDCl_3$): δ 5.78 (dq, $J = 15.2$, 6.4 Hz, 1H), 5.55 (dt, 15.2, 6.0 Hz, 1H), 5.30 (d, $J = 1.1$ Hz, 1H), 4.83 (d, $J = 4.5$ Hz, 1H), 4.69 (d, $J = 4.6$ Hz, 1H), 4.24 (dd, $J = 6.0$, 0.8 Hz, 1H), 4.01 (dd, $J = 7.1$, 0.8 Hz, 1H), 2.91 (d, $J = 7.9$ Hz, 1H), 2.50 (d, $J = 7.9$ Hz, 1H), 1.80-1.45 (m, 4H), 1.73 (d, $J = 6.4$ Hz, 3H) ppm; ^{13}C NMR ($CDCl_3$): δ 175.5, 131.2, 125.0, 105.5, 79.7, 79.0, 69.6, 50.4, 49.8, 28.0, 27.2, 17.3 ppm.

8b: yield 21 mg, 9%, mp 116–118 °C, ^{1}H NMR ($CDCl_3$): δ 5.76 (dq, $J = 15.3$, 6.4 Hz, 1H), 5.57 (m, 1H), 5.56 (d, $J = 6.8$ Hz, 1H), 5.11 (d, $J = 4.8$ Hz, 1H), 4.90 (d, $J = 4.7$ Hz, 1H), 4.35 (dt, $J = 5.5$, 1.3 Hz, 1H), 4.06 (m, 1H), 2.88 (d, $J = 8.4$ Hz, 1H), 2.67 (dd, $J = 6.9$, 8.1 Hz, 1H), 1.85–1.38 (m, 4H), 1.73 (d, $J = 6.5$ Hz, 3H) ppm; ^{13}C NMR ($CDCl_3$): δ 175.0, 130.6, 125.3, 102.1, 78.7, 76.0, 70.6, 51.2, 46.6, 27.6, 27.5, 17.2 ppm.

X-Ray Crystallography

Crystallographic data (MoKα, $2\theta_{max} = 50°$) were collected on an Oxford Diffraction Gemini S Ultra CCD diffractometer at 293 K. Data reduction and empirical absorption corrections were carried out with the CrysAlis Pro program (Oxford Diffraction vers. 171.33.42). The structure was solved by direct methods with SHELXS86 and refined with SHELXL97 [24]. All non-H-atoms were refined aniostropically and H-atoms were constrained at their estimated positions using a riding model. The thermal ellipsoid diagrams were generated with ORTEP3 [25]. All crystallographic calculations were carried out within the WinGX graphical user interface [26]. The crystal and instrumental parameters used in the unit-cell determination and data collection are summarized in Table 1.

Table 1 Crystal data and refinement details for (**7b**) and (**8a**)

	(**7b**)	(**8a**)
Formula	$C_{11}H_{14}O_4$	$C_{12}H_{16}O_4$
Formula weight	210.22	224.25
Temperature (K)	298	298
Wavelength (Å)	0.71073	0.71073
Crystal system	Triclinic	Monoclinic
Space group	$P\bar{1}$ (No. 2)	$P2_1/c$ (No. 14)
Unit cell dimensions		
a (Å)	4.8787(5)	16.926(1)
b (Å)	9.6866(8)	8.4182(4
c (Å)	11.1979(9)	8.1004(5)
α (°)	89.843(6)	
β (°)	79.465(7)	94.128
γ (°)	85.653(7)	
Volume (Å^3)	518.74(8)	1151.2(1)
Z	2	4
Density (calculated) (g cm^{-3})	1.346	1.294
Absorption coefficient (mm^{-1})	0.102	0.097
F(000)	224	480
Crystal size (mm)	0.3 × 0.2 × 0.08	0.4 × 0.4 × 0.1
θ range for data collection (°)	3.70–25.00	3.42–24.99
Reflections collected	3,289	4,181
Independent reflections	1,828	2,020
Observed reflections	979	944
R_{int}	0.0249	0.0367
Number of parameters	136	145
Goodness-of-fit on F^2	0.797	0.773
Final R indices [$I > 2\sigma(I)$]	$R_1 = 0.0360$, $wR_2 = 0.0609$	$R_1 = 0.0423$, $wR_2 = 0.0773$
R indices[all data]	$R_1 = 0.0876$, $wR_2 = 0.0673$	$R_1 = 0.178$, $wR_2 = 0.0871$
CCDC deposition no.	826792	826791

Results and Discussion

Our primary interest with Novo-6 was in the development of new structure activity relationship data through the synthesis of focused compound libraries, and we rationalised that this approach may also be used to simplify the separation of the diastereomers identified in Scheme 1. We hoped that the introduction of a hydrophobic tail would simplify chromatographic resolution. The C3-OH moiety results in a highly polar material with no R_f difference observed between isomers (0.35, 1:1 EtOAc:Hexanes). However, given the additional synthetic step to form the desired ether analogues, consideration must be given to the mechanism of addition. If the reaction proceeds via an acid catalysed S_N2 mechanism, then we would expect inversion of configuration, however if the reaction proceeded via an oxonium stabilised carbocation, no conclusion as to the stereochemistry of Novo-6 could be drawn. Regardless, obtaining crystals of the resultant products would allow assignment of the relative stereochemistry of the Novo-ether analogues, which in turn could assist in the design of new, more potent analogues.

In a typical experiment, the *p*-toluene sulfonic acid mediated substitution reaction produced both desired isomers as shown in Scheme 2. NMR examination of the crude reaction mixture showed the presence of two isomers in a 6:1 ratio. Flash silica chromatography allowed isolation of each isomer pairing (**7a**:**7b** and **8a**:**8b**).

Characterisation of the relative stereochemistry of each isomer was originally carried out by ^{1}H NMR analysis. Although the spectra were very similar, a change in coupling constant assigned to the hydrogen at position C3 was observed between isomers. The major isomer was always found to have a higher R_f (TLC, 0.81, 1:1 EtOAc:Hexanes) and produced a characteristic doublet with a coupling constant of $J = 1.7$ Hz whereas the minor isomer, with a lower R_f (0.62, 1:1 EtOAc:Hexanes), produced a doublet with a coupling constant, $J = 6.8$ Hz. This was originally explained by the varying bond angle and orbital overlap between the hydrogens at position **3** and **3a** between the two isomers depicted in Fig. 3. In order to confirm these observations, crystal structures of **7b** (Fig. 4) and **8a** (Fig. 5) each as racemates were determined.

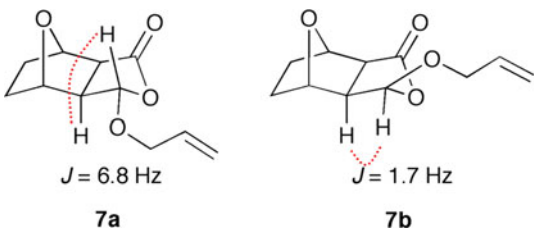

Fig. 3 Dihedral angle (°) and ^3J (Hz) difference between **7a** (110.7°) and **7b** (10.4°)

The conformation of **7b**, shown in Fig. 4, indicates that the allyloxy substituent is syn with respect to the furan O-atom (O2). The allyl group in this conformation is close to the bridgehead O-atom (O4), which based on an acid catalysed S_N2 mechanism is less favourable than the orientation shown for the major product **7a**, making this the less favoured isomer which correlates well with the observed yield of this isomer. The H–C3–C3a–H dihedral angle obtained from this crystal structure is 10.4° and supports the previously assigned NMR structure based on

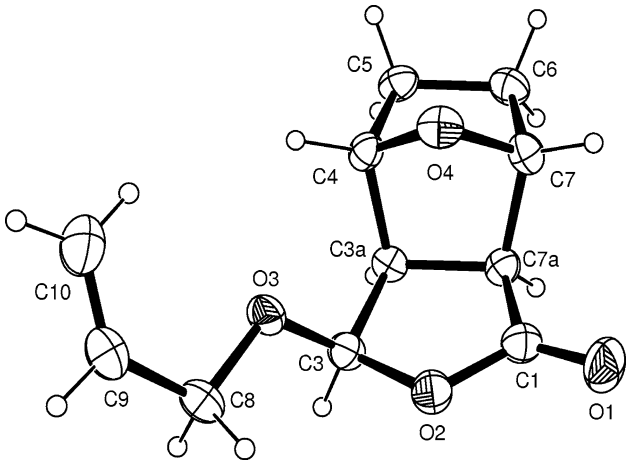

Fig. 4 ORTEP 3 view of **7b** (30% ellipsoids shown)

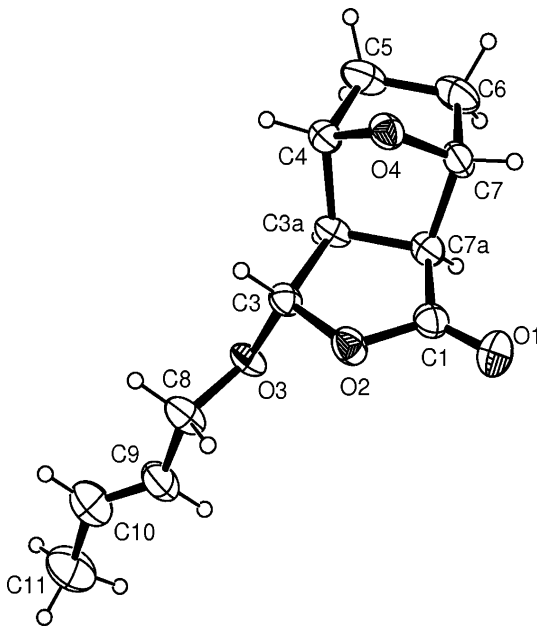

Fig. 5 ORTEP 3 view of **8a** (30% ellipsoids shown)

dihedral angle and orbital overlap between hydrogens at positions **3** and **3a**.

Compound **8a** was also crystallised. In this case the crotyl ether substitutent is anti with respect to the bridgehead O-atom. Of note is that the H-C3-C3a-H dihedral angle is 110.7°. This further confirms the observed ratio of anti:syn of 6:1 and stereochemical assignment from the structure of **7b**. Nucleophilic attack on C3 by the corresponding alcohol is far less hindered from below the plane compared to attack from above the plane of the Novo backbone due to the presence of large polar groups situated at the bridgehead and lactone group of the molecule.

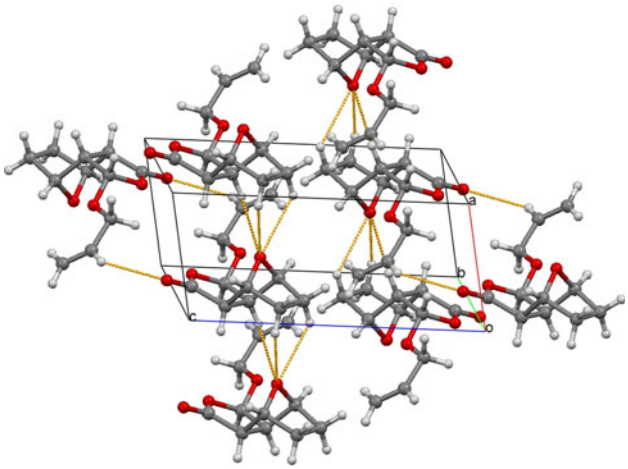

Fig. 6 Mercury (vers. 2.4) representation of the packing in **7b** highlighting non-classical H-bonding contacts

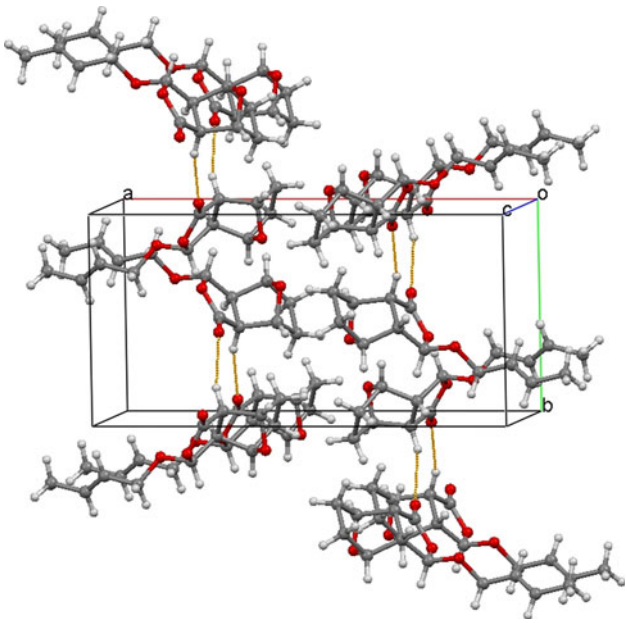

Fig. 7 Mercury (vers. 2.4) representation of the packing in **8a** highlighting non-classical H-bonding contacts

The packing diagram of **7b** is presented in Fig. 6 (generated with Mercury vers. 2.4) showing a number of weak non-classical C–H···O bonds (none closer than 2.6 Å).

A somewhat different packing is seen in **8a** and in this case the carbonyl O-atom is the only potential acceptor involved in significant non-classical H-bonds (C5–H···O2′ 2.54 Å: symmetry x, 3/2 − y, z − 1/2). The oxa bridgeheads of neighbouring molecules are pointing towards each other and the ether tails are pointing in the same direction, in contrast to the anti-parallel arrangement in **7b**.

In summary, two unsaturated Novo-6 analogues, **7** and **8**, have been synthesised, separated into their corresponding epimers and one example of each has been structurally characterised. The difference in configuration at position **3** (atom C8 in Fig. 4, 5) results in an observable change in ^{1}H NMR specifically the ^{3}J coupling between hydrogens at positions **3** and **3a**, respectively due to their very different dihedral angles. The ratio of isomers has been experimentally shown to be 6:1. The major isomer, with the ether tail orientated below the plane of the lactone ring, has far less orbital overlap and a ^{3}J coupling constant of $J = 1.7$ Hz corresponding to the hydrogens at positions **3** and somewhat different packing is seen in, respectively. The minor isomer with the ether tail orientated above the plane of the lactone ring, has a higher degree of orbital overlap resulting in a higher ^{3}J coupling constant of 6.8 Hz between hydrogens at positions **3** and **3a**, respectively (Fig. 7).

Acknowledgment The authors acknowledge the financial support of the Australian Research Council, the Australian Cancer Research and Ramaciotti Foundations, and John Morris Scientific, Australia. MT acknowledges the UNI-PRS postgraduate funding from the University of Newcastle.

References

1. Wang GS (1989) J Ethnopharmacol 26:147
2. Goldfarb MT, Gupta AK, Sawchuk WS (1991) Dermatol Clin 9:287
3. Nicholls LC, Teare D (1954) Poisoning by cantharides. Br J Med 2:1384–1386
4. Southcott CV (1989) Injuries from coleoptera. Med J Aust 151:654–659
5. Liu XH, Balzsek I, Comisso M, Legras S, Marion S, Quittet P, Anjo A, Wang GS (1995) Eur J Cancer 31A:953
6. McCluskey A, Bowyer MC, Collins E, Sim ATR, Sakoff JA, Baldwin ML (2000) Bioorg Med Chem Lett 10:1687
7. Corral JM, Gordaliza M, Castro MA, Lopez Vazquez ML, Garcia Gravalos MD, Broughton HB, Feliciano AS (1997) Tetrahedron 53:6555–6564
8. McCluskey A, Keane MA, Mudgee LM, Sim ATR, Sakoff J, Quinn RJ (2000) Eur J Med Chem 35:957–964
9. Lin PY, Shi SJ, Shu HL, Chen HF, Lin CC, Liu PC, Wang LF (2000) Bioorg Chem 28:266–272
10. McCluskey A, Walkom C, Bowyer MC, Ackland SP, Gardiner E, Sakoff JA (2001) Bioorg Med Chem Lett 11:2941–2946

11. Sakoff JA, Ackland SP, Baldwin ML, Keane MA, McCluskey A (2002) Investig New Drugs 20:1–11
12. McCluskey A, Keane MA, Walkon CC, Bowyer MC, Sim ATR, Young DJ, Sakoff JA (2002) Bioorg Med Chem Lett 12:391–393
13. McCluskey A, Ackland SP, Bowyer MC, Baldwin ML, Garner J, Walkom CC, Sakoff JA (2003) Bioorg Chem 31:68–79
14. Hart ME, Chamberlin RA, Walkom C, Sakoff JA, McCluskey A (2004) Bioorg Med Chem Lett 14:1969–1973
15. Baba Y, Hirukawa N, Sodeoka M (2005) Bioorg Med Chem Lett 13:5164–5170
16. Kok SHL, Chui CH, Lam WS, Chen J, Tang JCO, Lau FY, Cheng GYM, Wong RSM, Chan ASC (2006) Int J Mol Med 17:151–157
17. Kok SHL, Chui CH, Lam WS, Chen J, Lau FY, Wong RSM, Cheng GYM, Tang WK, Teo ITN, Cheung F, Cheng CH, Chan ASC, Tang JCO (2006) Int J Mol Med 18:1217–1221
18. Kok SHL, Chui CH, Lam WS, Chen J, Lau FY, Wong RSM, Cheng GYM, Tang WK, Cheng CH, Tang JCO, Chan ASC (2006) Int J Mol Med 18:375–379
19. Deng L, Shen L, Zhang J, Yang B, He Q, Hu Y (2007) Can J Chem 85:938–944
20. Hill TA, Stewart SG, Ackland SP, Gilbert J, Sauer B, Sakoff JA, McCluskey A (2007) Bioorg Med Chem 15:6126–6134
21. Stewart SG, Hill TA, Gilbert J, Ackland SP, Sakoff JA, McCluskey A (2007) Bioorg Med Chem 15:7301–7310
22. Hill TA, Stewart SG, Sauer B, Gilbert J, Ackland SP, Sakoff JA, McCluskey A (2007) Bioorg Med Chem Lett 17:3392–3397
23. Eggelte TA, De Koning H, Huisman HO (1973) Tetrahedron 29:2445–2447
24. Sheldrick GM (2008) Acta Crystallogr A A64:112–122
25. Farrugia LJ (1997) J Appl Crystallogr 30:565
26. Farrugia LJ (1997) J Appl Crystallogr 32:837